HEFAT2014
10th International Conference on Heat Transfer, Fluid Mechanics and Thermodynamics
14 – 16 July 2014
Orlando, Florida

NUMERICAL SIMULATION OF NATURAL CONVECTION IN A SPHERICAL POROUS ANNULUS

Sangita, M.K. Sinha, R.V. Sharma*
*Author for correspondence
Department of Mechanical Engineering
NIT Jamshedpur-831013
India
E-mail: rvsharma.me@nitjsr.ac.in

ABSTRACT

The present study reports results of numerical investigation of natural convection in a spherical annulus filled with fluid saturated porous medium. The inner and outer surfaces are maintained at low and high temperature respectively. Successive Accelerated Replacement (SAR) scheme has been employed to obtain numerical solution for wide range of parameters i.e Rayleigh number ($100 \le Ra \le 2000$) and aspect ratio ($0.25 \le A \le 1.0$). As Rayleigh number and aspect ratio increase, the average Nusselt number increases. The boundary layer formation takes place at higher Rayleigh number. The centre of the stream lines shift downwards as aspect ratio increases

INTRODUCTION

Natural convection in porous media is getting attention by researchers in the recent years owing to applications such as, insulation for cryogenic containers, disposal of nuclear waste material, design of pebble bed nuclear reactors, solar collectors, extraction of geothermal energy, high performance matrix heat exchangers, transpiration cooling, enhanced recovery of oil by thermal methods, buried pipelines, underground spread of pollutants, and storage of thermal energy.

Studies on flow over a sphere embedded in porous media have been reported. Padmavathi et al. [1], Berman [2] have studied the Stokes flow past a sphere embedded in a porous medium using continuity of velocity components as well as continuity of stress components. Srivastava and Srivastava [3] have discussed the steady flow of an incompressible viscous fluid streaming past a porous sphere at small Reynolds number with a uniform velocity. Grosan [4] et al. has studied steady flow of a viscous fluid past a permeable porous sphere embedded in another porous medium using the Brinkman equation model for the flow inside and outside the sphere.

Studies on natural convection in spherical porous annulus are limited. Burns and Tien [5] studied natural convection in porous media completely enclosed by concentric spheres up to Rayleigh number 75. Pop et al.[6] studied transient-free convection between two concentric spheres filled with a porous medium. Short-time solutions to the momentum and energy equations were obtained analytically using asymptomatic expansion method. Baytas et al. [7] studied steady natural convection in a porous medium bounded by concentric spherical annular sectors. Sangita et al. [8] studied natural convection in a spherical porous annulus employing Darcy-Brinkman flow model.

For the complete spherical porous annulus employing Darcy flow model, the available literature is by Burns and Tien [5] only and the results are limited up to Ra=75. So, there is a need for further study. The present study pertains to natural convection in a spherical annulus employing Darcy flow model with inner and outer surfaces maintained at cold and hot respectively. This has direct applications in design of storage for cold materials in spherical containers or cryogenic containers.

NOMENCLATURE

A	[-]	Aspect ratio
g	[m/s^2]	Acceleration due to gravity
r	[m]	Radial co-ordinate
R	[-]	Dimensionless radial co-ordinate
u, v	[m/s]	Velocity in r and ∅ direction
K	[m^2]	Permeability of porous medium
p	[N/m^2]	Fluid pressure
P	[-]	Dimensionless pressure
Ra	[-]	Rayleigh number
T	[K]	Temperature
θ	[-]	Dimensionless temperature
Nu	[-]	Local Nusselt number
$\overline{Nu}$	[-]	Average Nusselt number
Greek symbols		
α	[m^2/s]	Thermal diffusivity
β	[K^{-1}]	Coefficient of thermal expansion
∅	[rad]	Polar co-ordinate
ε	[-]	Error tolerance limit
μ	[N-s/m^2]	Dynamic viscosity of fluid
ω	[-]	Acceleration factor
ρ	[kg/m^3]	Fluid density
Ψ	[-]	Dimensionless stream function
θ	[-]	Dimensionless temperature
Subscripts		
c		cold
h		hot

i	inner
o	outer
m	mean
e	effective

MATHEMATICAL FORMULATION

The mathematical model for a steady two dimensional natural convection in a spherical porous annulus is presented. The inner cold and the outer hot walls are assumed to be at constant temperatures T_c and T_h respectively. The Physical model and co-ordinate system is shown in Figure 1. The flow is governed by Darcy law. Boussinesq approximation is valid. The fluid and solid matrix are in thermal equilibrium. Viscous dissipation and pressure work are negligible. Porous medium is isotropic and homogeneous.

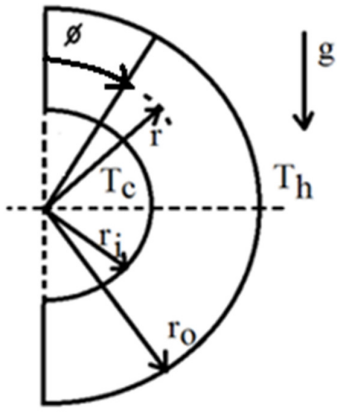

Figure 1 Physical model and co-ordinate system

With above assumptions, the governing equations consisting of conservation of mass, momentum and energy are given as,

$$\frac{\partial}{\partial r}(r^2 u \sin\phi) + \frac{\partial}{\partial \phi}(rv\sin\phi) = 0 \quad (1)$$

$$\frac{\mu}{K}u = -\frac{\partial p}{\partial r} - \rho g\cos\phi \quad (2)$$

$$\frac{\mu}{K}v = -\frac{1}{r}\frac{\partial p}{\partial \phi} + \rho g\sin\phi \quad (3)$$

$$u\frac{\partial T}{\partial r} + \frac{v}{r}\frac{\partial T}{\partial \phi} = \alpha\left(\frac{\partial^2 T}{\partial r^2} + \frac{2}{r}\frac{\partial T}{\partial r} + \frac{1}{r^2}\frac{\partial^2 T}{\partial \phi^2} + \frac{\cot\phi}{r^2}\frac{\partial T}{\partial \phi}\right) \quad (4)$$

Density variation according to Boussinesq approximation is given by,

$$\rho = \rho_m[1 - \beta(T - T_m)] \quad (5)$$

These equations are solve along with the following boundary conditions,

$$u = 0, T = T_c, T_h \text{ at } r = r_i, r_o \text{ for } 0 \le r \le \pi$$

$$v = 0, \frac{\partial T}{\partial \phi} = 0 \text{ at } \phi = 0, \pi \text{ for } r_i \le r \le r_o \quad (6)$$

Governing equations are rendered dimensionless introducing the following dimensionless variables,

$$R = \frac{r}{r_i},\ \theta = \frac{T - T_c}{T_h - T_c},\ U = \frac{ur_i}{\alpha},\ V = \frac{vr_i}{\alpha},\ P = \frac{pK}{\mu\alpha} \quad (7)$$

Equations (1) – (6) in non dimensional forms can then be written as

$$\frac{\partial}{\partial R}(UR^2\sin\phi) + \frac{\partial}{\partial \theta}(V\sin\phi) = 0 \quad (8)$$

$$U = -\left[\frac{\partial P}{\partial R} + \left(\frac{\rho_m g K D}{\mu\alpha}\right)\bar{\rho}\cos\phi\right] \quad (9)$$

$$V = -\left[\frac{\partial P}{R\,\partial \phi} - \left(\frac{\rho_m g K D}{\mu\alpha}\right)\bar{\rho}\sin\phi\right] \quad (10)$$

$$\frac{\partial^2\theta}{\partial R^2} + \frac{2}{R}\frac{\partial\theta}{\partial R} + \frac{1}{R^2}\frac{\partial^2\theta}{\partial\phi^2} + \frac{\cot\theta}{R^2}\frac{\partial\theta}{\partial\phi} = U\frac{\partial\theta}{\partial R} + \frac{V}{R}\frac{\partial\theta}{\partial\phi} \quad (11)$$

$$\bar{\rho} = 1 - \beta(T_h - T_c)(\theta - 0.5) \quad (12)$$

Pressure term is eliminated by differentiating equation (9) with respect to ϕ and equation (10) with respect to R, which simultaneously gives the equation,

$$\frac{\partial U}{\partial\phi} - V - R\frac{\partial V}{\partial R} = -\left(\frac{\rho_m g K r_i}{\mu\alpha}\right)\left[\frac{\partial\bar{\rho}}{\partial\phi}\cos\phi + R\frac{\partial\bar{\rho}}{\partial R}\sin\phi\right] \quad (13)$$

Introducing the stream function (ψ) which satisfies continuity equation and relates velocity components U and V as,

$$U = \frac{1}{R^2\sin\phi}\frac{\partial\psi}{\partial\phi} \quad (14)$$

$$V = -\frac{1}{R\sin\phi}\frac{\partial\psi}{\partial R} \quad (15)$$

Momentum equation (13) and energy equation (11) can be expressed in terms of stream function and temperature as,

$$R^2\frac{\partial^2\psi}{\partial R^2} + \frac{\partial^2\psi}{\partial\phi^2} - cot\phi\frac{\partial\psi}{\partial\phi} = RaR^3 sin\phi\left(\frac{\partial\theta}{\partial R}sin\phi + \frac{\partial\theta}{\partial\phi}\frac{cos\phi}{R}\right) \quad (16)$$

$$R^2 sin\phi\left(\frac{\partial^2\theta}{\partial R^2} + \frac{2}{R}\frac{\partial\theta}{\partial R} + \frac{1}{R^2}\frac{\partial^2\theta}{\partial\phi^2} + \frac{cot\phi}{R^2}\frac{\partial\theta}{\partial\phi}\right) = \frac{\partial\psi}{\partial\phi}\frac{\partial\theta}{\partial R} - \frac{\partial\psi}{\partial R}\frac{\partial\theta}{\partial\phi} \quad (17)$$

The boundary conditions on stream function and temperature are given by,

$$\psi = 0,\ \theta = 0 \ at\ R = 1 \ \ for\ 0 \le \phi \le \pi$$
$$\psi = 0,\ \theta = 1 \ at\ R = A + 1 \ \ for\ 0 \le \phi \le \pi$$
$$\psi = 0,\ \frac{\partial\theta}{\partial\phi} = 0 \ at\ \phi = 0, \pi \ for\ 1 \le R \le (A + 1) \quad (18)$$

Where, Rayleigh number (Ra) and aspect ratio (A) are defined as,

$$Ra = \frac{\rho_m g K\beta(T_h - T_c)r_i}{\mu\alpha} \quad (19)$$

$$A = \frac{r_o - r_i}{r_i}, \quad (20)$$

NUMERICAL SCHEME

Governing equations along with boundary conditions are solved by employing Successive Accelerated Replacement (SAR) scheme as described in [9]. The basic philosophy of the SAR scheme is to guess profile for each variable which satisfies boundary conditions. It is natural to associate the equation for each dependent variable, which contains the highest order derivative of that variable. For example, conservation of momentum equation is associated for correcting the profile of stream function and conservation of energy equation is associated for correcting the temperature profile.

Let the partial differential equation governing a stream variable and temperature are given by $\tilde{\psi}_{i,j}$ and $\tilde{\theta}_{i,j}$ at any mesh point i,j corresponding to R and $\emptyset$ positions respectively. The equation $\tilde{\psi}_{i,j} = 0$ and $\tilde{\theta}_{i,j} = 0$ are obtained using finite difference representation for the governing equations. The guessed profile in general will not satisfy the equations. The error arising in equation at n^{th} iteration be $\tilde{\psi}_{i,j}^{n}$ and $\tilde{\theta}_{i,j}^{n}$. The (n +1)th approximation to the variable ψ and θ are obtained from

$$\psi_{i,j}{}^{n+1} = \psi_{i,j}{}^{n} - \omega \frac{\tilde{\psi}_{i,j}{}^{n}}{\partial \tilde{\psi}_{i,j}{}^{n}/\partial \psi_{i,j}} \quad (21)$$

$$\theta_{i,j}{}^{n+1} = \theta_{i,j}{}^{n} - \omega \frac{\tilde{\theta}_{i,j}{}^{n}}{\partial \tilde{\theta}_{i,j}{}^{n}/\partial \theta_{i,j}} \quad (22)$$

The acceleration factor ω varies from 0 to 2. A set of convergence criteria is achieved by the correction of the variable at every mesh point. The criterion is,

$$\frac{\Sigma_i \Sigma_j |\psi_{i,j}{}^{n+1} - \psi_{i,j}{}^{n}|}{\Sigma_i \Sigma_j |\psi_{i,j}{}^{n+1}|} \leq \varepsilon \quad (23)$$

$$\frac{\Sigma_i \Sigma_j |\theta_{i,j}{}^{n+1} - \theta_{i,j}{}^{n}|}{\Sigma_i \Sigma_j |\theta_{i,j}{}^{n+1}|} \leq \varepsilon \quad (24)$$

The error tolerance limit ε is a small positive number.

Nusselt Number

Local Nusselt number at the inner and outer spherical surfaces can be calculated by,

$$Nu_i = -\frac{A}{A+1}\frac{\partial \theta}{\partial R}\Big|_{R=1} \quad (25)$$

$$Nu_o = -(A+1)\frac{\partial \theta}{\partial R}\Big|_{R=(A+1)} \quad (26)$$

Average Nusselt number is calculated by applying Simpson's 1/3rd rule on finite difference equation of local Nusselt Number.

RESULTS AND DISCUSSION

It is worth to optimize the acceleration factor, error tolerance limit and grid size before studying the effect of Rayleigh number and aspect ratio on flow fields, temperature fields and heat transfer. Table 1 shows the optimum values acceleration factor.

Table1: Optimum values of acceleration factor

Ra	ω
0-500	1
501-1000	0.5
1001-2000	0.3

Grid sensitivity test has been carried out and given in Table 2. A grid size of 60×60 is found to be optimum for all computations.

Table 2: Grid sensitivity test for $Ra = 1000, A = 1.0$

Grid size	$\overline{Nu}_i$	$\overline{Nu}_o$
50×50	7.53	7.44
60×60	7.44	7.39
70×70	7.41	7.36

The convergence criterion is achieved when the relative error between two consecutive iterations of the variables is less than 10^{-5}. The validation of present numerical result is performed against the work of Burns and Tien [5] and Baytas et al.[7] as shown in Table 3.The present results show agreement with the results.

Table 3: Validation of the present results of average Nusselt number, $\overline{Nu}$ with Burns and Tien [5] and Baytas et al. [7]

Ra	Burns and Tien [5] $\overline{Nu}$	Baytas et al. [7] $\overline{Nu}$	Present $\overline{Nu}$
10	1.06	1.04	1.04
30	1.36	1.31	1.26
50	1.74	1.70	1.57
75	2.10	2.11	1.94

Flow and Temperature Fields

Figures 2 & 3 show streamlines and isotherms for Ra=100 & 1000 at A=0.25 respectively. The intensity of the contour lines increases near the inner and outer circular wall of the sphere with increase of aspect ratio. Isotherms are almost circular arc at A=0.25 and it is distorted when A=1.0. So, it is clear that at lower aspect ratio the conduction is dominating phenomena.

Figures 4 & 5 show streamlines and isotherms for Rayleigh number 100 and 1000 respectively at aspect ratio A=1. It is depicted from the Figures 2 & 3 and Figures 4 & 5 that as Rayleigh number increases the bean shaped streamlines change its shape. It is depicted from the figures that the centre of the cell raises downward as Rayleigh numbers increase and the intensity of the contour lines increases near the inner and outer circular wall of the sphere. At the lower Rayleigh number, isotherms are almost circular arc. In this case, conduction heat transfer is dominating over

convection heat transfer. Figure 3 indicates distortion of isotherms as the Rayleigh number increases. At higher Rayleigh number, convection heat transfer is more dominant than that of conduction heat transfer.

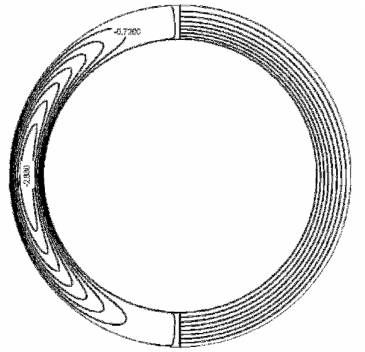

Figure 2 Streamlines (left) and isotherms (right) for Ra=100, A=0.25

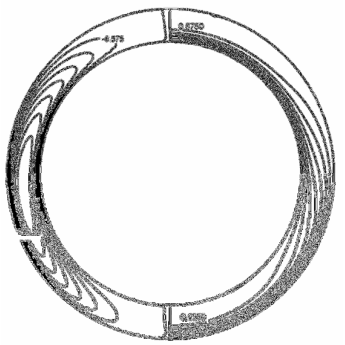

Figure 3 Streamlines (left) and isotherms (right) for Ra=1000, A=0.25

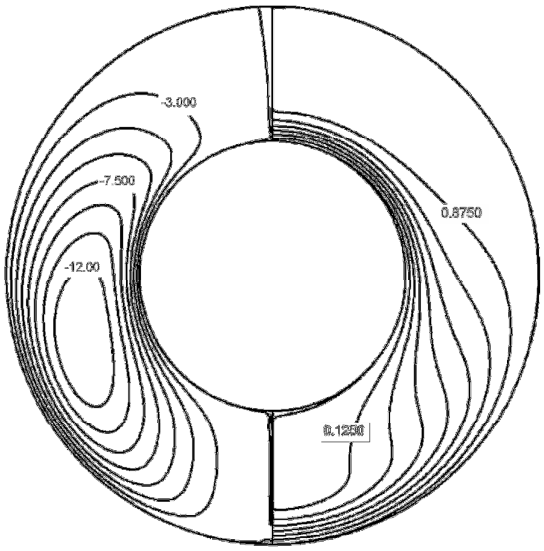

Figure 4 Streamlines (left) and isotherms (right) for Ra=100, A=1.0

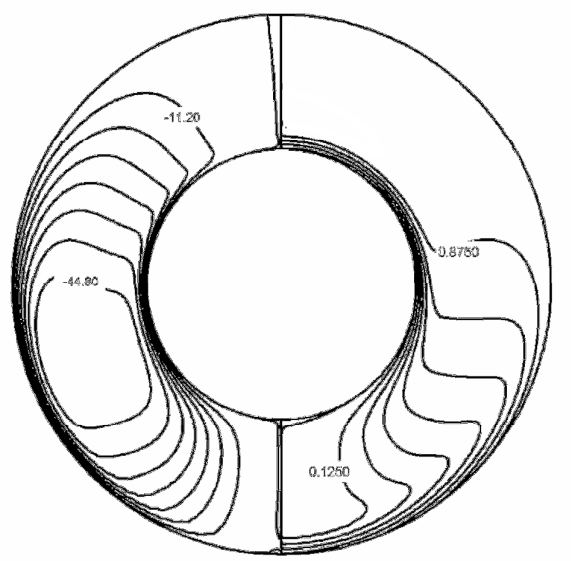

Figure 5 Streamlines (left) and isotherms (right) for $Ra = 1000, A = 1.0$

Heat Transfer Results

Figure 6 & 7 show variation of average Nusselt number with Rayleigh number and aspect ratio respectively. The average Nusselt number value increases with increase in Rayleigh number and aspect ratio.

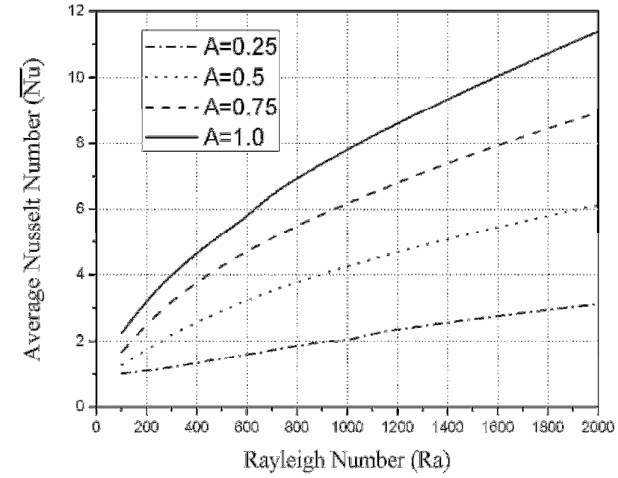

Figure 6 Plot of Average Nusselt number $(\overline{Nu})$ with Rayleigh number (Ra) at different aspect ratio

Figures 8 & 9 show plot of local Nusselt number with angular position. It is depicted from figures that the local Nusselt number value at the inner wall decreases with increase in angular position. Similarly, the local Nusselt number value at the outer wall of the spherical porous annulus increases with increase in angular position.

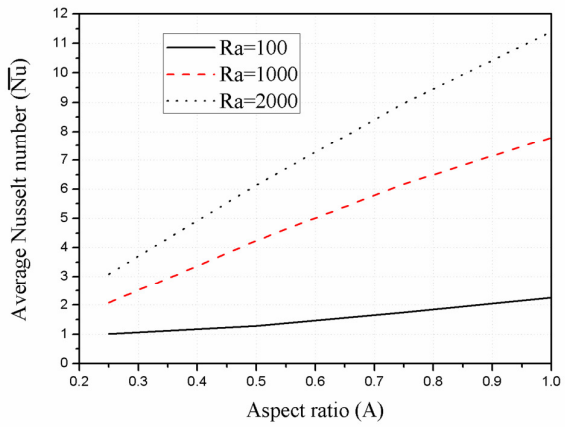

Figure 7 Plot of Average Nusselt number ($\overline{Nu}$) with aspect ratio

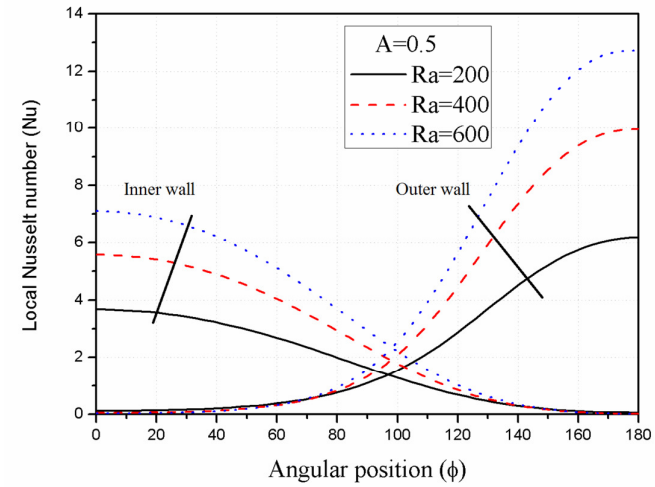

Figure 8 Plot of local Nusselt number (Nu) with angular position ($\emptyset$) for $Ra = 200, 400, 600$ at $A = 0.5$

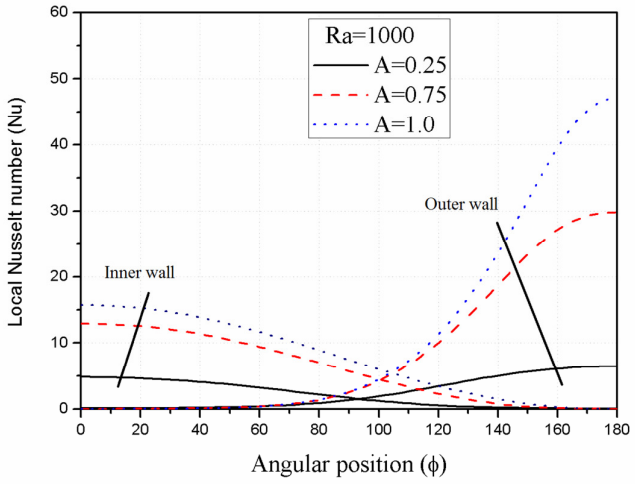

Figure 9 Plot of local Nusselt number (Nu) with angular position ($\emptyset$) for $A = 0.25, 0.75, 1.0$ at $Ra = 1000$

Correlation

A correlation has been developed relating average Nusselt number to Rayleigh number and aspect ratio by using Engineering Equation Solver (EES) software in which variable metric method of minimization is used. EES helps tremendously to develop such complicated correlations very easily. The correlation is as follows,

$$\overline{Nu} = a + (Ra^b)(c + dA + eA^2) \quad (27)$$

The correlation coefficients a, b, c, d and e are tabulated in the Table 4.

Table 4: The correlation coefficients of Equation (27)

correlation coefficients	values
a	0.1963
b	0.5643
c	-0.008051
d	0.1991
e	-0.03731

The above correlation is valid for 100≤Ra≤2000 and 0.25≤A≤1.0. Figure 10 shows that the value of average Nusselt number found by correlation is in agreement with numerical value.

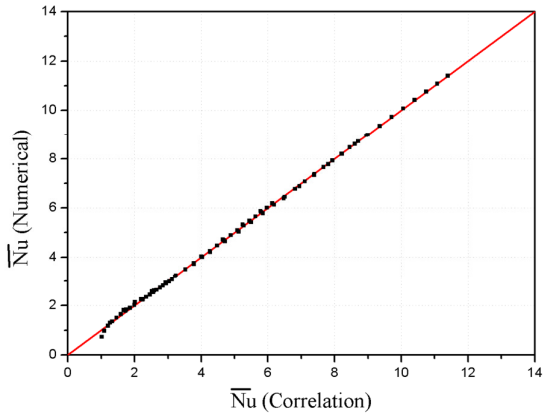

Figure 10 Plot of average Nusselt number ($\overline{Nu}$) found numerically vs. correlation

Comparison with results of fluid-filled enclosures

For a spherical annulus with r_i=1 m, r_o=1.25 m, T_c=-50°C, T_h=50°C, filled with glass wool with permeability K=10^{-7}m^2 and thermal conductivity $k_{porous} = 0.045 W/mK$

Thus, aspect ratio $A = \frac{r_o - r_i}{r_i} = 0.25$

Properties value of air at $T_m = 273$K,

$\rho_m = 1.293 Kg/m^3$, $\mu_{air} = 17.16 \times 10^{-6}\ Ns/m^2$,

$\alpha_{air} = 18.806 \times 10^{-6}\ m^2/s$, $k_{air} = 0.024 W/mK$,

$C_p = 1005\ J/KgK$

$\beta = 3.66 \times 10^{-3} K^{-1}$

Case I: Spherical annulus filled with air

As given by Scanlan et al.[10]

$$Ra^* = \frac{\rho_m g \beta (T_h - T_c)(r_o - r_i)^4}{\mu_{air} \alpha_{air}} = 28102301.74$$

$$\frac{k_{effective}}{k_{air}} = 0.228(Ra^*)^{0.226} = 10.998$$

Heat transfer by convection,

$$Q_c = \frac{4\pi k_{effective}(T_h - T_c) r_o r_i}{(r_o - r_i)} = 843.83 \text{ W}$$

Case II: Spherical annulus filled with air saturated porous media

$$\alpha = \frac{k_{porous}}{\rho_m C_p} = \frac{0.045}{1.293 \times 1005} = 3.23 \times 10^{-5} m^2/s$$

$$Ra = \frac{\rho_m g K \beta (T_h - T_c) r_i}{\mu_{air} \alpha} = 418.59$$

Numerically $\overline{Nu} = 1.38$

$$\overline{Nu} = \frac{k_{effective}}{k_{porous}}$$

$$k_{effective} = 0.0621 W/mK$$

Heat transfer by convection,

$$Q_c = \frac{4\pi k_{effective}(T_h - T_c) r_o r_i}{(r_o - r_i)} = 195.09 \text{W}$$

When above two cases are compared, it is clear that by filling fluid saturated porous media instead of only fluid reduces heat transfer drastically.

CONCLUSIONS

Numerical simulation has been carried out for natural convection in a spherical annulus filled with fluid saturated porous medium with inner and outer spheres maintained at cold and hot temperatures respectively. The flow and temperature fields in terms of streamlines and isotherms and heat transfer in terms of Nusselt number depend on two dimensionless parameters i.e. Rayleigh number (Ra) and aspect ratio (A). It has been found that as Rayleigh increases the value of average Nusselt number increases. Also, as the aspect ratio increases, the average Nusselt number increases. The centre of the stream lines shifted downward as aspect ratio increases for a given value of the Rayleigh number. Compared to fluid filled spherical annulus, use of porous material reduces convection heat transfer drastically.

REFERENCES

[1] Padmavathi B.S., Amaranath T., Nigam, S.D., Stoke's flow past a porous sphere using Brinkman model, Z. Angew. Math. Phys. vol.44, 1993, pp.929–939.

[2] Berman B., Flow of a Newtonian fluid past an impervious sphere embedded in a porous medium, Indian Journal of Pure and Applied Mathamatics, vol. **27**, 1996, pp. 1249–1256.

[3] Srivastava A.C., Srivastava N., Flow past a porous sphere at small Reynolds Number, Z. Angew. Math. Phys. vol. 56, 2005, pp. 821–835.

[4] Grosan T., Postelnicu A., Pop I., Brinkman flow of a viscous fluid through a spherical porous medium embedded in another porous medium, Transport in Porous Media vol. 81, 2010, pp.89–103.

[5] Burns, P. J. and Tien, C. L., Natural convection in porous media bounded by concentric spheres and horizontal cylinders, International Journal of Heat Mass Transfer, vol.22, 1979, pp.929–939.

[6] Pop, I., Ingham, D.B. and Cheng, P., Transient free convection between two concentric spheres filled with a porous medium, Journal of Thermo physics and Heat Transfer, vol.7, 1993, pp.724-727.

[7] Baytas, A. C., Grosan, T. and Pop, I., Free convection in spherical annular sectors filled with a porous medium, Transport in Porous Media, vol.49, 2002, pp.191–207.

[8] Sangita, Sinha M. K. and Sharma R. V., Natural convection in a spherical porous annulus: The Brinkman extended Darcy flow model, Transport in Porous Media vol.100, 2013, pp.321–335.

[9] Chandra P. and Satyamurty V.V., Non-Darcian and anisotropic effects on free convection in a porous Enclosure. Transport in Porous Media, vol. 90, 2011, pp.301–320.

[10] **S**canlan J. A., Bishop E. H. , Powe R. E., Natural convection heat transfer between concentric spheres, International Journal of Heat Mass Transfer, Vol. 13, 1970, pp. 1857-1872.

[11] Nield D.A. and Bejan, A., Convection in porous media, 3rd edition, Springer, New York, 2006.

[12] Vafai, K. (Ed.), Handbook of porous media, 2nd edition, New York, Taylor and Francis, 2005.

[13] Vadasz, P., Emerging topics in Heat and Mass transfer in porous media, Springer, New York, 2008.

[14] Ingham, D. B., Pop, I., Transport phenomena in porous media, Elsevier, Oxford, 2005.